

## 1. Materials and Reagents

### *Materials-Carnosinol synthesis and analytical chemistry*

Ultrapure water was prepared with a Milli-Q H<sub>2</sub>O purification system (Millipore, Bedford, USA). Solvents for HPLC and LC-MS and all the chemicals of analytical grade were purchased from Sigma–Aldrich (Milan, Italy). L-Carnosine and carnosinol were obtained from Flamma S.p.A. (Chignolo d'Isola, Italy). 4-Hydroxy-2-nonenal dimethyl acetal was synthesized according to the literature <sup>1</sup> and was stored at -20°C. For each experiment, fresh 4-hydroxy-2-nonenal was prepared as previously described <sup>2</sup>. Experimental determination of the lipophilicity parameters (log P and log D<sub>7.4</sub>) and ionization constants was performed by titration analyses by using the Sirius GIpKa apparatus as described in <sup>3</sup>. Chelation complexes with Cu<sup>2+</sup> were analyzed by titration analyses adding CuCl<sub>2</sub> at the same concentration of the titrated compound to the aqueous solution as reported by <sup>4</sup>. The obtained pH-metric data were analyzed using the BSTAC program (De Stefano, C.; Mineo, P.; Rigano, C.; Sammartano, S. Ionic strength dependence of formation constants. XVII. The calculation of equilibrium concentrations and formation constants. *Ann. Chim. (Rome)* 1993, 83, 243–277) in order to calculate the corresponding chelation constants.

## 2. In silico studies

The nucleophilicity parameter N<sup>5</sup> was derived based on DFT calculations as described in <sup>6</sup>. The resolved structure of CN1 was retrieved from PDB (Id: 3DLJ) and was initially prepared by removing water molecules and all crystallization additives. Since this structure includes a homodimer, the simulations involved the monomer B which is the monomer with less unresolved gaps (gaps: 77-79 and 208-209) and with the higher percentage of residues falling in the allowed regions of the Ramachandran plot (82.23 vs. 81.95). The included gaps were then filled by using the corresponding segments of the previously reported homology model <sup>7</sup> and the completed protein was firstly minimized by taking fixed all atoms apart from those included into a 8 Å radius sphere around the inserted segments followed by a minimization with backbone atoms fixed to optimize the overall protein structure preserving the experimental folding.

The obtained CN1 structure was then utilized in docking simulations to generate the complex with carnosine and carnosinol. In detail, docking calculations were performed by PLANTS (Korb, O.; Stütze, T.; Exner, T. E. (2009) Empirical Scoring Functions for Advanced Protein-Ligand Docking with PLANTS *J.Chem.Inf.Model.* 49, 84-96) focusing the search into a 10 Å radius sphere around the barycenter of the two zinc ions; each simulation generated 20 poses which were scored by the ChemPLP function with speed equal to 1. Best-fit complexes were finally minimized by taking fixed all atoms apart from those included into a 10 Å radius sphere around the bound ligands.

Docking simulations on hPepT1 involved the already published homology model <sup>8</sup> and were performed by PLANTS focusing the search into a 10 Å radius sphere around Tyr588 applying the same procedures as detailed above for CN1.

## 3. In vitro studies

### *Sequestering activity: HPLC analysis*

The reactivity of carnosinol and of the other sequestering agents toward HNE was directly evaluated by measuring the aldehyde consumption by HPLC–UV analysis as already reported <sup>9</sup>. The selectivity was evaluated by a similar approach, for which pyridoxal was used instead of HNE to represent an endogenous aldehyde. Samples were prepared by

incubating each sequestering agent with HNE or pyridoxal in 10 mM phosphate buffer, pH 7.4 for 24 h at 37 °C. The quenching activity towards MGO was also determined by HPLC-UV analysis as already reported <sup>10</sup>, and setting the PDA detector at  $\lambda=285$  nm, which corresponds to the maximum absorbance wavelength of MGO.

#### *Inhibition of ubiquitin carbonylation by MS based analysis*

The effect of carnosinol and of reference compounds in inhibiting protein carbonylation induced by HNE, MGO and MDA was tested by using an in vitro assay as already reported [2, 10, 11]. The test is based on ubiquitin as target protein and on orbitrap MS system for measuring the extent of ubiquitin modification. RCS concentrations were selected to yield approximately 50% of RCS-carbonylated ubiquitin. Results are reported as % of inhibition of protein carbonylation.

#### *MS-based analysis of RCS/quencher reaction products*

After 24 h incubation, all samples were diluted approximately 10-fold in water and were directly infused into the LTQ-Orbitrap XL. The ESI source (Thermo Scientific, Milan, Italy) was set as follows: spray voltage 3.5 kV, sheath gas 5, capillary temperature 275°C, capillary voltage 35 V, tube lens offset 120 V. The lock mass option was enabled. Most abundant peaks were fragmented to obtain MS/MS spectra by using a selection window of 2.5 m/z. We used both CID and HCD fragmentation (with AGC target=1x10<sup>4</sup> or 2x10<sup>5</sup>, respectively); fragmentation products were acquired by using the Orbitrap analyzer at a resolving power 100000 (FWHM at m/z=400). Chemical structures of the reaction products were assigned on the basis of the elemental composition obtained by the Xcalibur/Qual Browser software by using a 8 ppm tolerance. Proposed structures were then confirmed by MS/MS experiments. Fragment ion structures were generated by The HighChem—MassFrontier software (version 5.1, Thermo Scientific) that generated theoretical fragments according to both general chemistry rules and HighChem fragmentation library.

## **4. ADMET studies**

In vitro ADMET studies were performed by Nikem research (Milan, Italy) following standardized experimental protocols. In vivo studies were carried out in agreement with the Italian Law (D. L.vo 116/92). PK studies were performed by using fasted CD male rats (Charles River Laboratories, Calco, Italy). Carnosinol was administered by oral gavage (PO) at a dose of 45 mg/Kg or by i.v. bolus (caudal vein) at the dose of 3 mg/Kg. Serial sampling was performed by caudal vein at the following time points: i.v. 2, 10, 30, 60, 120, 240, 480 min and 24 h; PO: 5, 15, 30, 60, 120, 240, 480 and 24 hours. For plasma carnosinol measurement, 100  $\mu$ l of plasma were added to a 96 deep wells plate (Waters) containing 300  $\mu$ l of CH<sub>3</sub>CN spiked with 10  $\mu$ l of IS (D-istidinol, 1000 ng/ml). The plate was shaken for 15 min and centrifuged for 15 min at 3000 rpm at 15°C. Supernatants were transferred in new deep wells plate and analyzed by LC/MS/MS using the following eluents: phase A, ammonium formate 10 mM, phase B: CH<sub>3</sub>CN, gradient from 0 to 0.2 min 90% of B, from 0.2 to 0.6 min 40% of B, from 0.6 to 1.5 min 40% of B, from 1.51 to 2 min 90% of B flow 0.8 ml/min; Column Atlantis silica Hilic 2.1x50mm 3  $\mu$ m, inj volume 5  $\mu$ l, T column 45°C. MS analyses were performed with a TSQ Quantum Triple Quadrupole (Thermo Finnigan Italy, Milan, Italy) mass spectrometer fitted with an electrospray (ESI) interface operating in positive ion mode and with the following source parameters: capillary temperature, 240°C; spray voltage 3.2 kV; capillary voltage, 35 V; and tube lens voltage 106 V. A multiple reaction monitoring (MRM) method was set up for the quantitative analyses and based on the following transitions: Carnosinol m/z 213.1  $\rightarrow$  195.1+ 178.1+ 166.0+124.0+ 81.0; IS m/z 142

→ 124.02. Data analysis was performed by non Compartmental Analysis WinNonlin 5.1, linear trapezoidal, uniform weight.

Toxicological studies were performed by Cyathus Exquiere Italia (Milan, Italy). Male and female Sprague-Dawley rats of 7 weeks (Harlan, Italy) were used for the study. All animals were weighed on the day of each treatment. Clinical signs were monitored at regular intervals throughout the study in order to assess any reaction to treatment. At the end of the experiment all the animals were killed by inhalation of carbon dioxide. The experiment was carried on in agreement with the Italian Law (D. L.vo 116/92). The test compound was administered daily for seven days by oral gavage at a dose volume of 10 ml/kg body weight. The volume administered was adjusted on the basis of the body weight recorded immediately before administration. Animals were fed prior to dosing. Control rats received the vehicle only at the same volume. Animals were observed individually after dosing at least once during the first 30 minutes, periodically during the days of treatment (1-2-4-6h) for the following behavioral changes or ill-health: changes in skin, fur, eyes, occurrence of secretion and excretions, lacrimation, piloerection, unusual respiratory pattern, change in gait, posture and response to handling, behavior pattern, stereotypies, bizarre behavior. Body weight and food consumption were determined at days 1, 3 and 8. Terminal Observation: On day 8 animals were weighed, sacrificed by inhalation of carbon dioxide and subjected to gross necropsy. At necropsy, appearance of superficial tissue and internal organs were carefully evaluated. All changes were recorded. Before the sacrifice, a retroorbital bleeding was performed for each animal under halothane anaesthesia to allow haematology and blood chemistry assays. Blood was collected in tubes for serum preparation and tubes containing EDTA as anticoagulant.

## **In vitro ADME studies**

### **Summary**

Carnosinol was determined to be completely stable in both simulated gastric fluid (pH= 1) and simulated intestinal fluid (pH = 7.4) and metabolically stable in rat plasma where the %-total remaining was  $101.4 \pm 3.6$  after 60 min of incubation. Carnosinol stability was then tested in human serum where it was found completely stable at least up to 60 min (% remaining of  $104.4 \pm 3.3$ ) while carnosine was totally consumed at the same experimental conditions, thus indicating that carnosinol is not recognized by carnosinases. The metabolic stability of Carnosinol was then evaluated in rat and human liver microsomes where the % remaining was of  $90.8 \pm 1.6$  and  $72.7 \pm 0.1$  as well as in rat and human S9 liver fraction ( $84.1 \pm 0.3$  and  $90.6 \pm 1.2\%$ ), demonstrating a good metabolic stability.

Carnosinol showed negligible or no inhibition of the most important isoenzymes (CYP1A2, CYP2C9, CYP2C19, CYP2D6 and CYP3A4) of cytochrome P450. The cytotoxic potential of Carnosinol was evaluated on human hepatoma cell line (HepG2). Carnosinol did not show any cytotoxic effect on human hepatoma cell line (HepG2) up to 100  $\mu$ M concentration (data not shown). The potential interaction of Carnosinol with the cardiac hERG K<sup>+</sup> channel was evaluated at 10  $\mu$ M concentration and no interaction with hERG binding at the concentration tested was observed.

### **4.1 Stability in Simulated Gastric Fluid (SGF) and Simulated Intestinal Fluid (SIF)**

The stability of Carnosinol was evaluated in Simulated Gastric Fluid (SGF, pH 1) and Simulated Intestinal Fluid (SIF, pH 7.4). Results obtained are reported in Table S1. Carnosinol showed a high stability in the SIF and the SGF up to 60 min of incubation. The

reference standard compounds are in agreement with literature and with internal validation data.

Compound	SIF	SGF
	% remaining at 60 min	
Carnosinol	115.5 ± 3.8	103.6 ± 0.6
Chlorambucil	18.8 ± 0.8	105.7 ± 10.3
Erythromycin	101.2 ± 2.5	3.9 ± 0.1
Rifampicine	101.5 ± 4.3	65.6 ± 1.3

**ADMET Table S1.** Percentage remaining after 60 min of incubation (SIF and SGF). Results are expressed as Mean with S.D., n=4

Stability of test compounds was compared to that of three known reference standards as reported in Table S2.

Compound	SIF		SGF	
	% Remaining at 1 h	Classification	% Remaining at 1 h	Classification
Rifampicin	95 ± 5	Stable	65 ± 5.0	Unstable
Chlorambucil	25 ± 7	Very Unstable	95 ± 5.5	Stable
Erythromycin	95 ± 5	Stable	6 ± 5	Very unstable

**ADMET Table S2.** Stability of standards and classification. Results are expressed as Mean ± S.D. n=4

#### 4.2 Stability in human and rat serum

The rat and human serum stability of Carnosinol was evaluated after 60 min incubation. Stability was calculated as percentage remaining of the area ratio compound/I.S. at each time point vs. area ratio compound/I.S. at time 0 min and the results are reported in Table S3. Carnosinol was stable in human and rat species at 60 min incubation. The standard reference compounds (Lidocaine and Sigma M7319) gave the expected stability.

Compound	Human	Rat
	% remaining at 60 min	
Carnosinol	105.4 ± 3.3	110.4 ± 3.6
Lidocaine	103.1 ± 4.1	88.4 ± 6.4
M7319	0.7 ± 0.1	1.9 ± 0.9

Results are expressed as Mean ± S.D.,  
n=2

**ADMET Table S3.** Serum stability results

Classification for categorizing compounds is reported in Table S4.

<b>%Remaining</b>	>80	80-60	60-30	<30
<b>Classification</b>	Stable	Slightly unstable	Unstable	Very unstable

**ADMET Table S4.** Plasma stability classification

#### 4.3 Metabolic stability in human and rat liver microsomes (Phase I)

The metabolic stability of Carnosinol was evaluated in rat and human liver microsomes to estimate the stability to phase I oxidative metabolism.

The results obtained are shown in Table S5. Carnosinol showed a good stability in human and rat liver microsomes. The metabolic stability of the standards compound 7-ethoxycoumarin and propranolol are in agreement with the literature and internal validation data.

Compounds	Human	Rat
	% remaining at 30 min	
Carnosinol	90.8 ± 1.6	72.7 ± 0.1
7-EC	5.9 ± 0.1	2.9 ± 0.9
Propranolol	48.2 ± 0.5	2.5 ± 0.2

**ADMET Table S5.** Metabolic stability data. Results are expressed as Mean ± S.D., n=4. Metabolic stability: >95:High; 50-95: Good; 10-50: Medium; <10:Low

#### 4.4 Metabolic stability studies in S9 liver fraction (Phase I, II)

The metabolic stability of Carnosinol was evaluated in rat and human S9 liver fraction, in presence of Phase II cofactors, to estimate stability to phase I and phase II metabolism. The results obtained are shown in Table S6. Carnosinol showed a good stability in S9 liver fractions in both rat and human species. The % remaining of the standard compounds 7-ethoxycoumarin and Propranolol were in agreement with the literature and internal validation data.

Compound	Human	Rat
	% remaining at 30 min	
Carnosinol	84.1 ± 0.3	90.6 ± 1.2
7-EC	27.5 ± 5.8	9.5 ± 0.3
Propranolol	70.5 ± 5.2	0.1 ± 0.1

**ADMET Table S6.** Metabolic stability studies in S9 liver fraction. Results are expressed as Mean ± S.D., n=4

#### 4.5 Inhibition of P450 enzymes at 10 $\mu\text{M}$

The interaction of Carnosinol with the on the most important isoenzymes (CYP1A2, CYP2C9, CYP2C19, CYP2D6 and CYP3A4) of cytochrome P450 enzymes was tested at 10  $\mu\text{M}$  concentration. Results are shown in Table S7 and table S8 (standard compounds).

Compound	CYP1A2	CYP2C9	CYP2C19	CYP2D6	CYP3A4
	CEC	MFC	CEC	AMMC	BFC
	Mean % inhibition at 10 $\mu\text{M}$				
Carnosinol	<5	<5	13.5 $\pm$ 3.3	<5	7.9 $\pm$ 1.1

**ADMET Table S7.** P450 results. Results are expressed as Mean  $\pm$  S.D., n=4; a <5% inhibition is considered no effect

Carnosinol showed negligible or no inhibition on all isoforms while the standard reference inhibitors showed the expected potency.

Cytochrome	Standard	IC <sub>50</sub> $\mu\text{M}$
1A2	Furafylline	2.3 $\pm$ 0.2
2C9	Sulfaphenazole	0.26 $\pm$ 0.04
2C19	Tranilcypromine	10.0 $\pm$ 0.4
2D6	Quinidine	0.0052 $\pm$ 0.0010
3A4	Ketoconazole	0.009 $\pm$ 0.001

**ADMET Table S8.** P450 results on standard inhibitors. Results are expressed as Mean  $\pm$  SD, n=4

#### 4.6 Cytotoxicity on HepG2

The cytotoxic potential of Carnosinol was evaluated on human hepatoma cell line (HepG2). The results obtained are shown in Table S9.

Carnosinol did not show any cytotoxic effect up to 100  $\mu\text{M}$  concentration while the reference standards (Terfenadine and Clozapine) showed the expected potency.

Compound	HepG2
	LC <sub>50</sub> , $\mu\text{M}$ (Mean $\pm$ S.D.)
Carnosinol	>100
Terfenadine	5.4 $\pm$ 0.1
Clozapine	40.1 $\pm$ 0.5

**ADMET Table S9.** Cytotoxicity results. Results are expressed as Mean  $\pm$  S.D., n=4

#### 4.7 Cytotoxicity in fluctuation assay

Carnosinol was tested in fluctuation assay testing the compound on one *Salmonella* strain to verify its potential cytotoxicity.

The assay is based on the ability of compounds to induce reverse mutation in point mutation made *ad hoc* in the histidine locus of different *Salmonella* strains. These bacteria normally are not able to growth in absence of exogenous histidine. Since Carnosinol is a dipeptide alanine-histidine, the capability of the tester strains to utilise it as histidine source was evaluated.

Cytotoxicity studies were performed on *S. typhimurium* TA100, the most sensitive strain among those utilized in the fluctuation assay. Carnosinol did not show any cytotoxic effect up to 5 mg/ml concentration (Table S10).

To check if Carnosinol could be utilized as histidine source, the *S. typhimurium* TA98 strain was preferred, presenting a lower spontaneous reversion (Table S11).

In addition to a mutation in the histidine operon, the tester strains contain another mutation that enhances their sensitivity to some mutagenic compounds. The mutation is the *uvrB* deletion, that results in a deficient DNA excision repair system, and that extend also through the *bio* gene. For this last reason the Ames strains require biotine for growth.

Compound	S. Typhimurium TA100	
	MIC µg/ml	
	NB	MM
Carnosinol	>5000	>5000
Ampicillin	256	512
Novobiocin	1	2

**ADMET Table S10.** MIC results. Inoculum: 10<sup>6</sup> CFU/ml

In Table S11 the positive control is the MM added with the two aminoacids, the negative control is MM without histidine and biotine, where no growth is expected, whereas in the case bio+ his- growth is possible only if the strain can utilize Carnosinol as histidine source. This occurs from 5 mg/ml to 5 µg/ml; for this reason the Ames assays does not appear to be a suitable test for this compound both in agar and broth format.

The reference standards ampicillin and novobiocin showed the expected potency.

Compound	S. Typhimurium TA98		
	MIC µg/ml		
	MM bio <sup>+</sup> his <sup>+</sup>	MM bio <sup>+</sup> his <sup>-</sup>	MM bio <sup>-</sup> his <sup>-</sup>
Carnosinol	>5000	Growth up to 5	ng
Ampicillin	256	ng	ng
Novobiocin	4	ng	ng

ng: no visible growth

**ADMET Table S11.** MIC results

#### 4.8 Cardiac hERG K<sup>+</sup> channel in vitro binding

The potential interaction of Carnosinol with the cardiac hERG K<sup>+</sup> channel was evaluated at 10 µM concentration. The results obtained are reported in Table S12.

Carnosinol did not display any interaction with hERG binding at the concentration tested.

The standard astemizole, tested in the same experiment, showed the expected K<sub>i</sub> value.

Compound	Mean %B ± S.D.
Carnosinol (10 µM test concentration)	104.4 ± 8.0
	Mean K <sub>i</sub> , nM
Astemizole	2.5 ± 0.3

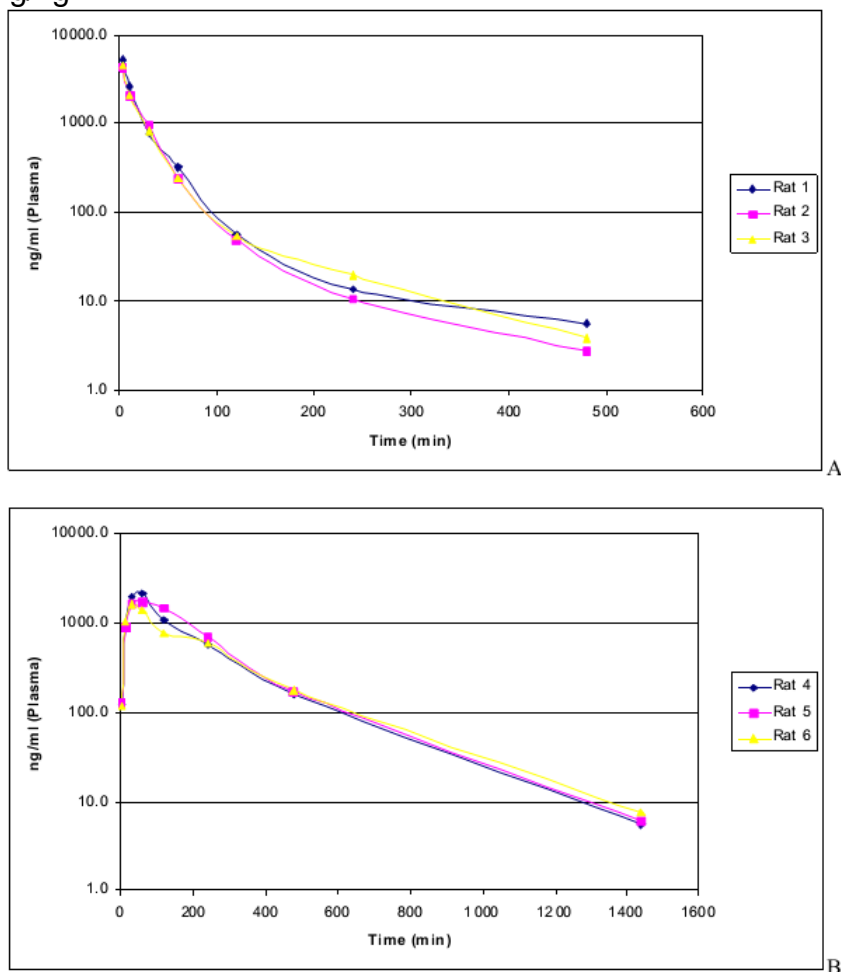
**ADMET Table S12.** [<sup>3</sup>H]-Astemizole/hERG binding assay. Results are expressed as Mean ± S.D. n=2

### In vivo pharmacokinetic properties

Carnosinol showed a medium-low clearance in the rat after IV administration (29 ml/min/kg) with high distribution volume (Figure S1, upper panel).

T<sub>1/2</sub> calculated from the elimination phase of the IV kinetic is about 1.5 h, but it is probably underestimated due to the lack of the 24 h time point because concentration of the test item was below the LLOQ.

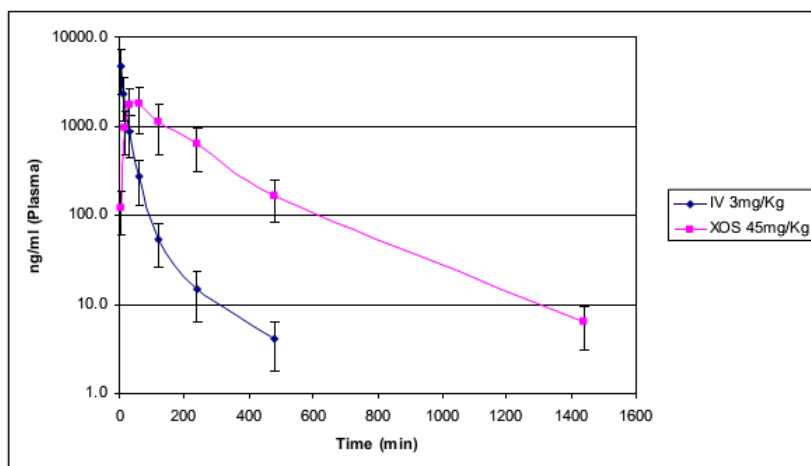
Oral profile (Figure S2, lower panel) showed T<sub>max</sub> at 1 h with a longer Mean Residence Time (MRT) of 219 min in respect to IV administration. The product resulted with an oral bioavailability calculated on AUC<sub>inf</sub> of 29%. Therefore Carnosinol showed a moderately good oral bioavailability giving a significant exposure in plasma after oral administration at the dose of 45 mg/kg.



**ADMET Figure S1.** Kinetic profiles of Carnosinol in plasma after IV administration (3 mg/kg, panel A) and after oral administration (45 mg/kg, panel B) in the rat

The comparison of the mean plasma kinetic profiles after IV and oral administration is reported in Figure S2.





**ADMET Figure S2.** Comparison of the mean plasma kinetic profiles of Carnosinol after IV and oral administration in the rat

## Toxicological profile

### 4.9. Maximum tolerated dose (MTD)

The study was performed to investigate the MTD (maximum tolerated dose) in male and female rats, after single oral administration of Carnosinol.

*In vivo* observations included survival, clinical signs, body weight, food consumption for 24 hours after the administration of Carnosinol.

Rats were treated orally with three different doses: 1.0, 1.5 and 2.0 g/kg. No evidence for gross adverse effects was observed in rats receiving 1.0, 1.5 g/kg of Carnosinol; all parameters were comparable to those of the control group.

Dose level of 2.0 g/kg Carnosinol resulted in modest body weight loss associated with a reduced food consumption.

No relevant gross findings were observed after 24 hours for all the treated rats excluding some little change in the colour of the glands on the surface of the stomachs of the two rats treated at 2.0 g/kg. However, with this dose, a tendency to produce some alterations in the animal welfare was noted thus, the MTD can be considered the dose tested of 1.5 g/kg.

### 4.10. Seven Days tox

This study was performed to investigate the subchronic toxicity in male and female rats, after seven days repeated oral administration of Carnosinol. Doses to perform this preliminary experiments were chosen taking into account the results of the MTD (maximum tolerated dose) study where the dose of 1.5 g/kg was supposed to be the MTD. The study was designed to test three dosages: MTD, 50% MTD and 25% MTD. However, the limited amount of test item available at the time of the experiment allowed to test the MTD and 50% MTD doses only. Haematology and blood chemistry were included in the study design as well as the gross macroscopic pathology. Organs were weighted if body weight was abnormal and abnormal organs or others were retained for possible histological studies that are not included in this study.

*In vivo* observations included survival, clinical signs, body weight, food consumption for 24 hours after the last administration of Carnosinol.

Rats were treated orally with two different doses: 0.75 and 1.5 g/kg. No evidence for gross adverse effects were observed in rats receiving Carnosinol. Increase of body weight was not significantly altered in both male and female groups treated at both doses of 1.5 g/kg

and 0.75 g/kg. The subchronic treatment did not influenced significantly the food consumption.

No relevant post-mortem gross findings were observed after 24 hours from the last administration in all the treated rats; liver and kidneys resulted mostly unaltered.

Blood chemistry data showed that treatment with Carnosinol up to 1.5 g/kg did not cause significant changes.

## 5. Rodent models of obesity/metabolic syndrome

### 5.1 Carnosinol in Fructose-fed rat model

Male Sprague-Dawley rats (Harlan Laboratories Inc., Udine, Italy) of 8 weeks of age and weighing  $200 \pm 20$  g were used for the study. Rats were housed under constant environmental conditions, with standard laboratory rat chow or 60% high fructose diet obtained from Mucedola s.r.l., Settimo Milanese, Milan, Italy and tap water ad libitum. In particular, the control diet contained 60% corn starch (carbohydrates), 20% casein (protein), 0.3% methionine, 5% lard (fat), 8% cellulose, 5% mineral mixture and 1% vitamin mixture, and zinc carbonate 0.004%. The fructose diet contained all the ingredients except corn starch, which was replaced by an equal quantity of fructose. Animals were acclimatized for a period of at least seven days before the use. The study was approved by the Animal Ethics Committee of University of Milan, Italy and communicated to the Italian Ministry of Health, corresponding to article seven of the D.L. 116/92.

Experimental design: rats were randomly divided into five groups. Control group (CTR group) received a standard rat chow diet for six weeks, whereas the other four groups were given fructose-enriched diet for six weeks. After three weeks the starting of the fructose diet, two groups were treated with carnosinol at two doses: 10 and 45 mg/kg/die. An additional group was treated with 10 mg/Kg/die of rosiglitazone (Glaxo-Smith-Klein, Middlesex, UK) which was found an effective therapeutic agent in this animal model (Cannizzaro et al, *Nutrition & Metabolism*, (2017) 14:5) and the fifth group continued with fructose-enriched diet alone (Hi fructose group). RGZ was orally administered by gastric gavage to rats during the last three weeks of the study while carnosinol was dissolved in the water diet. During all the experiments, rats had free access to water and food.

Plasma TNF- $\alpha$  and IL-6 were determined by ELISA using a commercially available kit (R&D Systems, Inc., USA) according to the manufacturer's instructions. Systemic blood pressure, Aspartate aminotransferase (AST), alanine transaminase (ALT), hepatic total lipids, hepatic triglycerides and hepatic total cholesterol were measured as previously described<sup>12</sup>. Plasma AGEs determined as carboxymethyl lysine (CML), carboxyethyl lysine (CEL) levels were measured by the use of commercially available kit: ELISA kit (OxiSelect™ CML ELISA Kit, Cell Biolabs Inc., OxiSelect™ CEL ELISA Kit, Cell Biolabs Inc.).

The levels of 8-epi-prostaglandin F2 $\alpha$  (8-epi-PGF2 $\alpha$ ; a marker of oxidative stress) in urine were measured using the enzyme immunoassay according to the manufacturer's instructions (Cayman kit, item n. 516351, Ann Arbor, MI, USA). Serum C reactive protein was determined by ELISA kit (Sigma- Aldrich, Milan Italy).

4.2 *Carnosinol in high fat, high sucrose (HFHS) fed WT and GPx4<sup>+/-</sup> mice.* Animal care and experimental procedures were performed with approval from the institutional animal care and use committee of East Carolina University and were in compliance with the National Institutes of Health's Guide for Care and Use of Laboratory Animals. C57BL6/J female mice (Jackson Laboratory) were crossed to male GPx4<sup>+/-</sup> mice and pups were genotyped by polymerase chain reaction (PCR) using primers described in<sup>13</sup>. At 8-12

weeks, WT and GPx4<sup>+/-</sup> male age-matched littermates were randomly assigned to groups and individually housed. Mice were fed either control (CNTL-TD110367) or high fat high sucrose (HFHS-TD110365) diet from Harlan-Teklad Laboratories (Madison, WI) *ad libidum* for 25 weeks. The composition of this diet was a special formulation consisting of mixed saturated and n-6 PUFA (44.6% kcal/g fat), with high sucrose (34% kcal/g) content<sup>14</sup>. After 8 weeks of HFHS diet, half of the HFHS diet-fed mice cohort (WT and GPx4<sup>+/-</sup>) were administered carnosinol (45 mg/kg/day) in their drinking water until study termination at 20 weeks. This dose was calculated based on a series of days where water consumption was meticulously recorded, and dose of carnosinol was maintained and adjusted to each mouse throughout duration of the study, according to its body weight. Mice were housed at controlled temperature and a 12hr light/dark cycle was maintained. At week 16 during the diet +/- drug intervention, live animal metabolic and echocardiographic measurements were made, including a cohort from each group (N=4) undergoing 5 days testing in the indirect calorimetry metabolic cage (TSE Systems, Chesterfield, MO). These measurements were done ~2-3 weeks prior to tissue collection to allow for a 'wash-out period' to minimize artifact attributable to additional stress that may have been introduced by these procedures.

**5.3. Metabolic Parameters.** Body weight of the mice was recorded on weekly basis throughout HFHS diet. Body composition was analyzed by nuclear- MRI (EchoMRI 700 Echo Medical Systems, Houston, TX). An oral glucose tolerance test (dose-0.5g/kg) was performed following a ~4 hour fast in week 22 of the HFHS diet period. Glucose levels were measured using a standard glucometer (OneTouch UltraMini, LifeScan, Milpitas, CA) in blood collected from a tail nick. Serum lipids were analyzed using UniCel DxC 600 (Beckman Coulter, Indianapolis, IN).

**5.4. 2-deoxyglucose (2-DOG) uptake in Soleus and EDL.** 2-DOG uptake was performed as previously described<sup>15</sup>. Briefly, soleus or EDL muscles were incubated with 200  $\mu$ U/ml of regular insulin or without insulin (basal). Muscles were incubated in Krebs-Henseleit buffer (KHB) + 0.1% bovine serum albumin (BSA) + 2 mM sodium pyruvate + 6 mM mannitol for 15 min, then transferred to a 2<sup>nd</sup> vial with KHB + 0.1% BSA + 1 mM 2-DOG (containing 2-deoxy-[<sup>3</sup>H]glucose, 6 mCi/mmol), + 9 mM mannitol (containing [<sup>14</sup>C]mannitol, 0.053 mCi/mmol) for 15 min. Samples were then processed, frozen, homogenized, and 2-DOG uptake was determined.

**5.5. Liver Histology.** Mice were anesthetized with isoflurane. Livers (n=2/group) were dissected and fixed in formaldehyde and embedded in paraffin wax. Tissues were cut cross-sectionally, stained in Hematoxylin and eosin or picosirius red (collagen), then viewed under polarized light. Liver steatosis was visualized with oil red O staining of liver triglycerides. Images of each heart were captured at 200X.

**5.6. Real-time qPCR of gene expression.** Liver samples (~10mg) were homogenized in glass grinders (Kimble Chase, Vineland, NJ). All materials used in RNA extraction were provided in RNeasy® Tissue Mini Kit (Qiagen Inc, Valencia, CA cat# 74704). Reverse Transcription was performed using the iScript™ cDNA Kit (Biorad Laboratories, Hercules, CA cat# 170-8891). The SsoAdvanced™ SYBER® Green reaction cocktail was used in the amplification and detection of DNA in RT-PCR. All protocols were performed according to product specifications unless otherwise stated. Cycle threshold (C(t)) values were converted to relative gene expression levels using the 2- $\Delta\Delta$ C(t) method and normalized to the level of Hypoxanthine-guanine phosphoribosyltransferase (HPRT) RNA. Data are reported as fold-change in gene expression (arbitrary units)  $\pm$  S.E.M. relative to WT-CNTL

mice (n=4-5 per group). The sequences and references for the primers used in qRT-PCR are listed in <sup>13</sup>.

**5.7. Protein extraction and immunoblot analysis.** Tissue samples were homogenized in TEET Buffer (10 mM Tris, 1 mM EDTA, 1 mM EGTA + 0.5% Triton X-100), then loaded on 4-20% pre-cast polyacrylamide SDS gel (Biorad, Hercules, CA) under reducing conditions. Protein was transferred to PVDF membranes (Millipore, Bellerica, CA) and incubated with primary antibodies for  $\alpha$ -tubulin (Abcam, Cambridge, UK),  $\beta$ -actin (Cell Signaling Technology, Danvers MA), and HNE-adduct (Percipio Biosciences). Membranes were incubated with infrared fluorophore-conjugated secondary antibodies (LiCor Biosciences, Lincoln, NE), scanned using Odyssey Clx Infrared Imaging System (Li-Cor) and analyzed by densitometry using Image J (NIH).

**5.8 Soluble and insoluble hydroxyproline content.** Liver samples were thawed and then suspended in 0.75 mL of phosphate-buffered saline (pH 3). Pepsin (Sigma-Aldrich) was then added to each sample at an amount of 40  $\mu$ g pepsin/milligram of tissue. Suspensions were gently shaken at 37°C for a period of 60 minutes, after which 0.75 mL of 2% SDS, 0.6M  $\beta$ -mercaptoethanol solution was added to each suspension. Suspensions were then vigorously sonicated for 30 minutes to allow soluble material to go into solution. These were then centrifuged at a high speed for 3h at 4°C. The insoluble fraction formed a visible pellet which contained the insoluble fraction of collagen, and the supernatant contained the soluble fraction of collagen. The supernatants were decanted into labelled glass test tubes and the insoluble fractions were resuspended in 0.5 mL of distilled water and also transferred to labelled glass test tubes. Samples were then dried in a heating oven. The residual film was hydrolyzed in 6.0 M HCl for 24 hours, dried, and resuspended in 50% isopropyl alcohol solution. Samples were then oxidized by 10  $\mu$ L addition of chloramine-T for ~5 minutes. To each sample, 50  $\mu$ L of a solution of 4-dimethylaminobenzaldehyde in 60% perchloric acid was then added before storing samples in the dark for 18 hours. Total hydroxyproline content within each fraction was then measured against a standard curve of known hydroxyproline (Sigma-Aldrich) by the procedure described in <sup>16</sup>. Hydroxyproline levels were normalized to protein concentration for each sample.

## **6. LC-MS analysis of carnosinol and carnosinol-aldehyde adducts in tissues**

### **6.1 Chemicals and sample preparation**

Water HPLC grade (18M $\Omega$ ) was purified with a Milli-Q water system (Millipore; Milan; Italy), HPLC grade solvents, TFA, PBS were purchased from Sigma Aldrich (Milan; Italy); Carnosinol was provided by Flamma s.p.a. (Chignolo D'Isola; BG; Italy). Tissue homogenates were prepared at the final concentration of 0.1mg tissue/ 1 mL PBS, by using a BeadBug tissue homogenizer (Benchmark Scientific, USA). The homogenization was done at 4°C to avoid enzyme activation and degradation of the analytes of interest. For each animal group, pooled samples were prepared by mixing equal-volume aliquots of individual samples.

Before analysis, samples were de-proteinized for 10 minutes at 4°C with 9 volumes of acetonitrile than centrifugated for 10 minutes at 14000 rpm at 4°C. Supernatants were collected and stored at -80°C before the analysis.

### **6.2 Synthesis of carnosinol-HNE adduct**

HNE was obtained by hydrolysis of the corresponding HNE-DMA in HCl 1mM for 1h at room temperature. HNE-DMA was synthesized as reported from Rees and colleagues <sup>17</sup>. Carnosinol-HNE adduct was then synthesized by mixing carnosinol and HNE at the final concentration of 1mM for 3h at 37°C in PBS (10mM).

### 6.3 Tissue distribution of Carnosinol.

Aliquots of 10µL of supernatants were sampled by the autosampler of an Exion™ LC 100 system (AB Sciex; MI; Italy). The chromatographic separation was carried out with a Thermo-Scientific Hypersil GOLD HILIC column (150x2.1mm, 3µM, 175Å). The flow rate was set at 250 µL/min and the column oven set at 40°C. As mobile phases were used-ammonium formate (100mM, pH 3, corrected with formic acid) and acetonitrile, with a gradient program reported in LC-MS Table 1.

LC-MS Table 1- Gradient program for chromatographic runs on HILIC column.

Time (min)	A ammonium formate 100mM pH 3(%)	B acetonitrile (%)
0.00	5.00	95.00
0.20	5.00	95.00
6.70	70.00	30.00
9.70	70.00	30.00
9.71	5.00	95.00
15.00	5.00	95.00

An API4000™ triple quadrupole analyzer equipped with a TurboV™ electrospray source (AB Sciex; MI; Italy) was used as detector. The mass spectrometer was working with the following source condition: +2.5kV ionization potential, 25 units of curtain gas, 40 units of gas 1 and 60 units of gas 2 heated at 550°C. Detector was in MRM mode, to monitor the transitions reported in LC-MS Table 2. Transitions were previously obtained by direct infusion of a standard solution of carnosinol at the final concentration of 20µM and parameters were optimized in a semi-automatic mode. During the analysis, collision gas was set at 4 units, declustering potential at 45 units, entrance potential at 10 units, collision cell exit potential at 10 units, and scanning time at 100ms for all the scans. Instrument control and data extraction were made by Analyst® 1.6.3 (AB SCIEX, MI+, Italy).

LC-MS Table 2- MRM transition for carnosinol quantification.

Parent ion (m/z)	Product ion (m/z)	Collision Energy (V)
213.2	178.1	24
213.2	166.3	24

### 6.4 Carnosinol-HNE tissues stability

Carnosinol-HNE adduct was added to blank tissue homogenates (heart, kidney, liver and PBS as control) at the final concentration of 5µM. Both carnosinol-HNE and homogenates were pre-warmed at 37°C prior incubation. XµL aliquots were sampled after 0,5,15,30,60,120 minutes and directly deproteinized at 4°C for 10 minutes with 9 volumes

of acetonitrile. Sample supernatants were then obtained as previously described and analyzed with the same method described above. In detail the MS analyzer was working in MRM mode to monitor the transition shown in LC-MS Table 3.

*LC-MS Table 3- MRM transition for quantification of carnosinol-HNE adduct.*

Parent ion (m/z)	Product ion (m/z)	Collision Energy (V)
369.4	334.2	32
369.4	166.3	40

### 6.5 Carnosinol-RCS adduct determination

Supernatants were dried under vacuum with an RVC 2–18 rotational vacuum concentrator (Christ, Germany) and re-dissolved in TFA 1% aqueous solution, to have 2-fold final dilution of the tissues homogenate. Samples were then placed in a 96-well plate for the analyses and stored in the autosampler at 8°C before the automatic injection.

The analytical platform consisted of an Ultimate 3000 nano LC system coupled with an LTQ-Orbitrap XL mass spectrometer through a Finnigan NSI-1 dynamic probe equipped with a stainless-steel LC/MS emitter as nanoelectrospray ionization source (5 cm length, O.D. 150 µm, I.D. 30 µm, Thermo Scientific, Rodano, MI, Italy). Aliquots of 10 µL of samples were injected automatically by the autosampler in a µ-Precolumn Cartridge (PrepMap100 C18, 0.3 x 5mm, 5 µm, 100Å Dionex) for sample wash and cleaning at 10 µL/min as flow rate of the loading pump with the following solvents composition 99% A (0.1% TFA) 1% B (ACN 0.1%FA). After 2 minutes the precolumn was diverted online to an Hypersil Gold Capillary Column (C18, 100 x 0.18 mm, 5µm, 175Å Thermo Scientific) at the flow rate of 1.5 µL/min following the gradient reported in LC-MS Table 4.

*LC-MS Table 4- Gradient program for reverse phase microscale LC-MS runs.*

Time (min)	A Water 0.1% FA (%)	B ACN 0.1%FA (%)
0.00	95	5
3.00	95	5
21.00	5	95
25.00	5	95
25.01	95	5
30.00	95	5

Ionization was performed in positive ion mode with 1.8kV source voltage, 220°C as capillary temperature, 35V capillary voltage, 110V tube lens. During the analysis the MS spectra were acquired in profile mode by Orbitrap using the following settings: scan range 250–700 m/z,  $5 \times 10^5$  ions per scan, maximum inject time was set to 500 ms, resolution was set to 100000 (FWHM at m/z 400). Lock mass option was enabled to provide a real time internal mass calibration during the analysis using as reference a list of 20 abundant and known background signals already reported by Keller and colleagues, as common air contaminants in mass spectrometry<sup>18</sup>. Instrument control was provided by the software Xcalibur 2.0 and Chromeleon Xpress 6.8 (Thermo Scientific, Rodano, MI, Italy).

## References

1. Siakotos, A. N., Schnippel, K., Lin, R. C. & Van Kuijk, F. J. Biosynthesis and metabolism of 4-hydroxynonenal in canine ceroid-lipofuscinosis. *Am. J. Med. Genet.* **57**, 290-293 (1995).
2. Colzani, M. *et al.* A novel high resolution MS approach for the screening of 4-hydroxy-trans-2-nonenal sequestering agents. *J. Pharm. Biomed. Anal.* **91**, 108-118 (2014).
3. Vistoli, G. *et al.* Predicting the physicochemical profile of diastereoisomeric histidine-containing dipeptides by property space analysis. *Chirality* **24**, 566-576 (2012).
4. Bertinaria, M. *et al.* Synthesis, physicochemical characterization, and biological activities of new carnosine derivatives stable in human serum as potential neuroprotective agents. *J. Med. Chem.* **54**, 611-621 (2011).
5. Domingo, L. R., Rios-Gutierrez, M. & Perez, P. Applications of the Conceptual Density Functional Theory Indices to Organic Chemistry Reactivity. *Molecules* **21**, 10.3390/molecules21060748 (2016).
6. Vistoli, G. *et al.* Computational approaches in the rational design of improved carbonyl quenchers: focus on histidine containing dipeptides. *Future Med. Chem.* **8**, 1721-1737 (2016).
7. Vistoli, G., Pedretti, A., Cattaneo, M., Aldini, G. & Testa, B. Homology modeling of human serum carnosinase, a potential medicinal target, and MD simulations of its allosteric activation by citrate. *J. Med. Chem.* **49**, 3269-3277 (2006).
8. Pedretti, A. *et al.* Modeling of the intestinal peptide transporter hPepT1 and analysis of its transport capacities by docking and pharmacophore mapping. *ChemMedChem* **3**, 1913-1921 (2008).
9. Vistoli, G. *et al.* Exploring the space of histidine containing dipeptides in search of novel efficient RCS sequestering agents. *Eur. J. Med. Chem.* **66**, 153-160 (2013).
10. Colzani, M. *et al.* Reactivity, Selectivity, and Reaction Mechanisms of Aminoguanidine, Hydralazine, Pyridoxamine, and Carnosine as Sequestering Agents of Reactive Carbonyl Species: A Comparative Study. *ChemMedChem* **11**, 1778-1789 (2016).
11. Colzani, M., Criscuolo, A., Casali, G., Carini, M. & Aldini, G. A method to produce fully characterized ubiquitin covalently modified by 4-hydroxy-nonenal, glyoxal, methylglyoxal, and malondialdehyde. *Free Radic. Res.* **50**, 328-336 (2016).
12. Aldini, G. *et al.* The carbonyl scavenger carnosine ameliorates dyslipidaemia and renal function in Zucker obese rats. *J. Cell. Mol. Med.* **15**, 1339-1354 (2011).
13. Katunga, L. A. *et al.* Obesity in a model of gpx4 haploinsufficiency uncovers a causal role for lipid-derived aldehydes in human metabolic disease and cardiomyopathy. *Mol. Metab.* **4**, 493-506 (2015).
14. Fisher-Wellman, K. H. *et al.* Novel role for thioredoxin reductase-2 in mitochondrial redox adaptations to obesogenic diet and exercise in heart and skeletal muscle. *J. Physiol.* **591**, 3471-3486 (2013).
15. Funai, K. *et al.* Skeletal Muscle Phospholipid Metabolism Regulates Insulin Sensitivity and Contractile Function. *Diabetes* **65**, 358-370 (2016).
16. Bondjers, G. & Bjorkerud, S. Spectrophotometric determination of hydroxyproline in connective tissue on the nanogram level. *Anal. Biochem.* **52**, 496-504 (1973).
17. Rees, M. S., van Kuijk, F. J. G. M., Siakotos, A. N., & Mundy, B. P. Improved synthesis of various isotope labeled 4-hydroxyalkenals and peroxidation intermediates. *Synthetic Communications*, **25**(20), 3225-3236 (1995).
18. Keller, B.O., Sui, J., Young, A.B., Whittall, R.M. Interferences and contaminants encountered in modern mass spectrometry. *Anal Chim Acta*, Oct 3; 627(1):71-81 (2008)

**Supplemental Table 1** – Comparison of lipophilicity, chelation and stereo-electronic properties between L-carnosine and carnosinol.

Compound	pK1	pK2	pK3	logP	logD <sub>7.4</sub>	CuHL pK	CuL pK	Rotors	N (1/ω)
Carnosine	2.76	9.33	6.72	0.23	-0.23	13.31	8.48	5	0.99
Carnosinol	---	9.19	6.69	0.44	0.28	12.73	5.49	6	1.39

Ionization and chelation constants as well as lipophilicity parameters were experimentally determined by titration analyses. Nucleophilicity index was computed by DFT simulations while the number of rotors is a well-known flexibility descriptor.



**Supplemental Table 2**– Reactivity of L-carnosine and Carnosinol with Acrolein & HNE

Buffer Rx	<i>Residual amount % (n=3)</i>					
	HNE			ACR		
	1h	2h	3h	1h	2h	3h
PBS	100.9 ± 2.2	103.0 ± 0.6	101.6 ± 1.8	90.4 ± 5.5	78.5 ± 6.8	68.8 ± 4.8
L-Carnosine	82.9 ± 5.0	70.9 ± 3.5	59.5 ± 3.2	33.1 ± 1.1	22.7 ± 5.7	22.4 ± 5.5
Carnosinol	69.9 ± 4.0	49.5 ± 3.5	35.4 ± 4.3	21.5 ± 1.8	13.3 ± 1.3	9.8 ± 1.2

Residual amount of acrolein (ACR) and 4-hydroxynonenal (HNE) from 50 µM initial concentration as determined by HPLC-UV (mean ± S.D.), at successive time-points following incubation with 1 mM Carnosine (CAR) or Carnosinol (COL) in 10 mM phosphate buffer (PBS), pH 7.4.

**Supplemental Table 3-** Metabolic and cardiovascular parameters from high fructose fed rats +/- Carnosinol.

	<i>Control Diet</i>	<i>Hi Fructose</i>	<i>Hi Fruc + Carnosinol (10 mg/kg)</i>	<i>Hi Fruc + Rosiglitazone (10 mg/kg)</i>	<i>Hi Fruc + Carnosinol (45 mg/kg)</i>
Initial body weight (g)	230.3±5.4	233.3±4.8	228.0±4.8	224.2±4.1	222.7±4.7
Final body weight (g)	406.5±9.9	447.3±9.8	432.8±10.3	413.4±10.7	420.7±13.1
Food intake (g/day)	24.5±2.2	27.3±2.8	25.8±2.6	23.8±2.3	25.3±2.4
Water intake (ml/day)	63.2±6.5	81.0±5.9	78.5±6.5	70.4±5.2	72.5±6.5
Systolic blood pressure (mmHg)	127.2±1.1	150.7±1.5†	146.8±1.4†	139.6±2.7†§*	135.3±2.2†§*
Heart rate (beats/min)	327.5±10.3	298.7±12.3	305.3±9.7	318.8±10.7	314.2±12.8
Heart weight (g)	1.19±0.06	1.27± 0.05	1.23±0.06	1.30±0.10	1.14±0.08

Data shown are mean ± S.E.M. and are from N=6 per group; †P<0.01 vs. Control Diet; §P<0.01 vs. Hi Fructose; \*P<0.01 vs. Hi Fruc + Car (10 mg/kg)

**Supplemental Table 4-** Plasma lipids and insulin levels in WT and GPx4<sup>+/-</sup> mice

	WT			GPx4 <sup>+/-</sup>		
	<u>CNTL</u>	<u>HFHS</u>	<u>HFHS+Car</u>	<u>CNTL</u>	<u>HFHS</u>	<u>HFHS+Car</u>
Triglycerides (mg/dL)	48.3 ± 2.8	42.8 ± 4.6	33.6 ± 2.9†	48.4 ± 1.1	31.5 ± 2.0†	26.5 ± 2.7†
Cholesterol (mg/dL)	57.7 ± 0.7	76.3 ± 6.2†	62.0 ± 7.5	57.0 ± 1.1	60.8 ± 6.1	47.5 ± 9.4
Insulin (ng/ml)	0.29 ± 0.1	0.43 ± 0.1	0.32 ± 0.07	0.38 ± 0.1	0.65 ± 0.1	0.5 ± 0.1

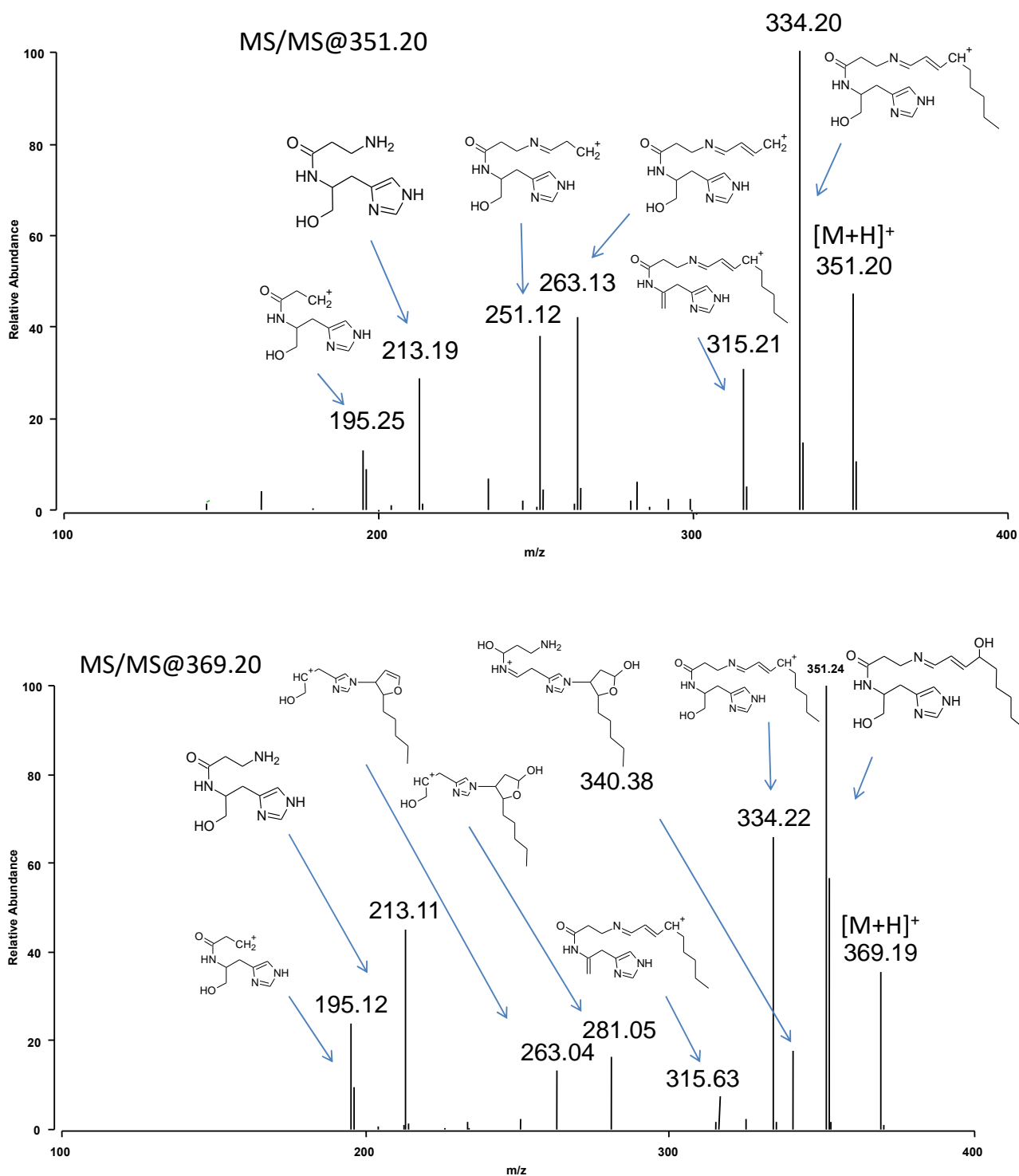
Data shown are mean ± S.E.M and are from N=6 per group; †P<0.05 vs. Control Diet within the genotype.

**Supplemental Table 5** – Free Carnosinol concentrations in Tissues

	WT			GPx4 <sup>+/-</sup>		
	<u>CNTL</u>	<u>HFHS</u>	<u>HFHS+Car</u>	<u>CNTL</u>	<u>HFHS</u>	<u>HFHS+Car</u>
Tibialis Anterior	≤ L.D.	≤ L.D.	≤ L.D.	≤ L.D.	≤ L.D.	≤ L.D.
Gastrocnemius	≤ L.D.	≤ L.D.	≤ L.D.	≤ L.D.	≤ L.D.	≤ L.D.
Pancreas	≤ L.D.	≤ L.D.	≤ L.D.	≤ L.D.	≤ L.D.	≤ L.D.
Liver	≤ L.D.	≤ L.D.	4.34 ± 0.3	≤ L.D.	≤ L.D.	3.59 ± 0.4*
Kidney	≤ L.D.	≤ L.D.	31.86 ± 4.5	≤ L.D.	≤ L.D.	22.95 ± 2.0*
Adipose tissue	≤ L.D.	≤ L.D.	0.19 ± 0.0	≤ L.D.	≤ L.D.	0.3 ± 0.02*

Data are from pooled samples from each genotype and treatment group (N = 4 per group);  
\*P<0.05 for genotype effect. L.D. = limit of detectability

## Supplemental Figure 1



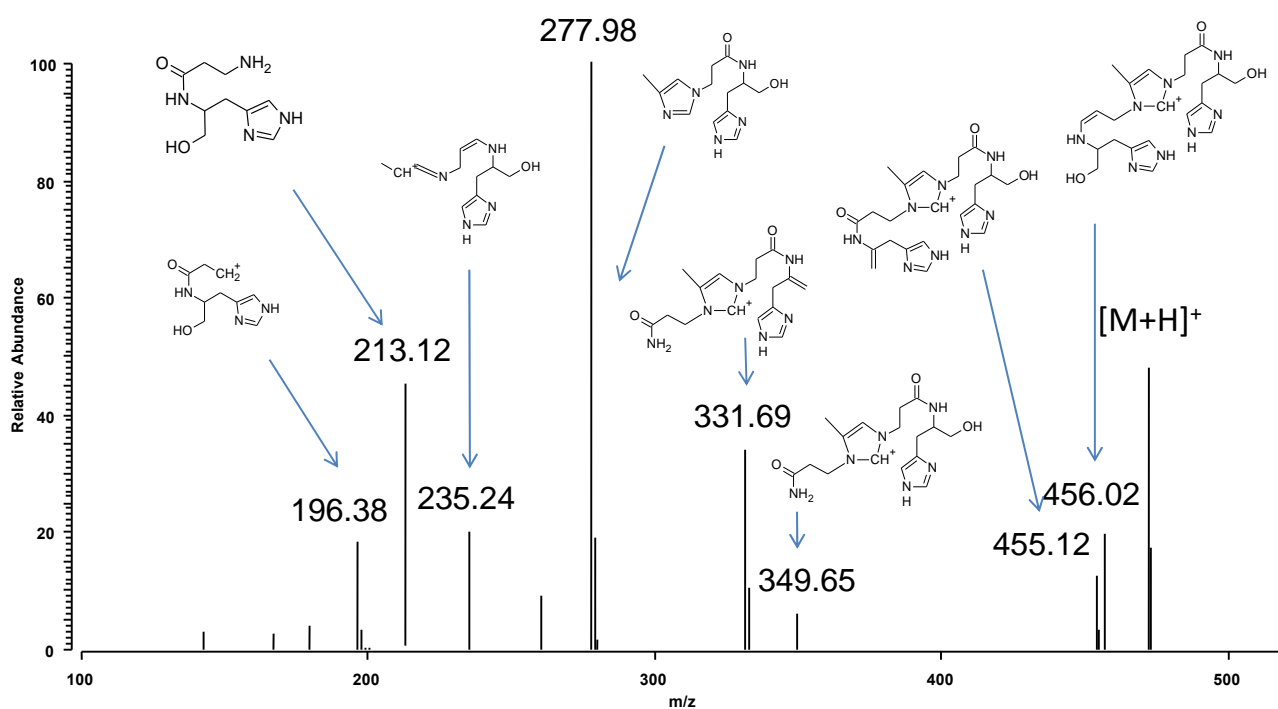
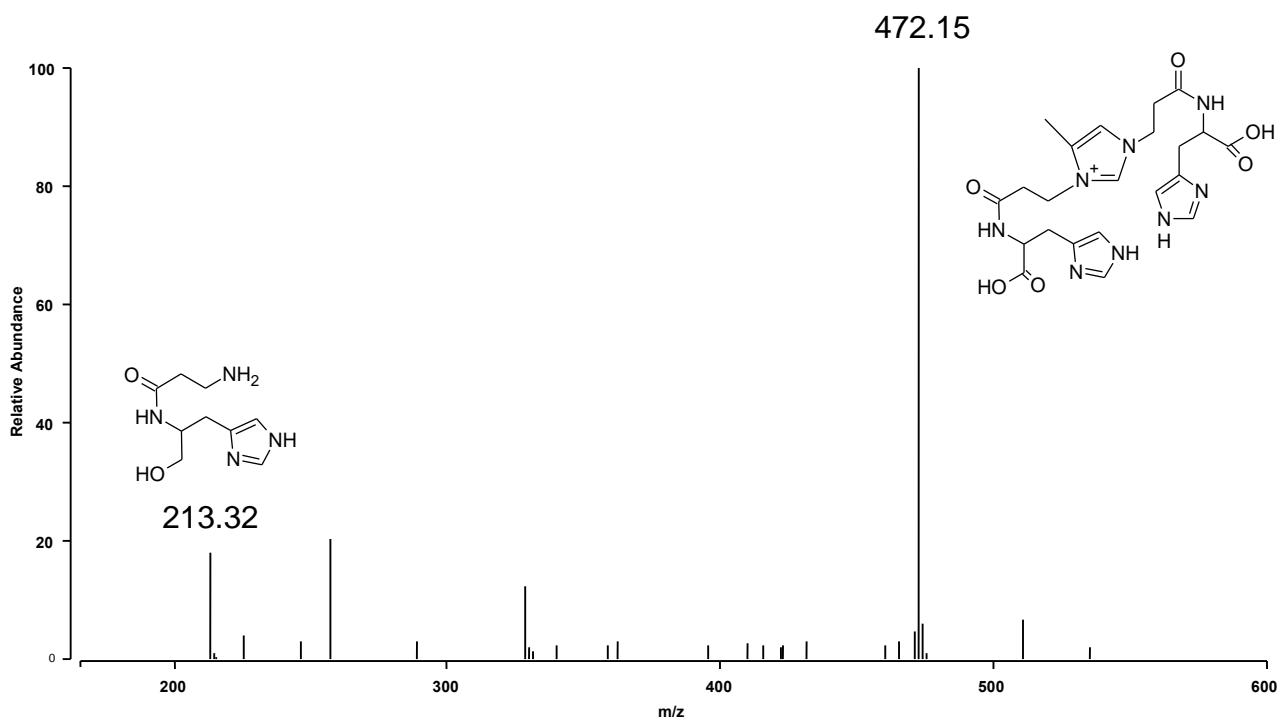
**Supplemental Figure 1. Carnosinol-HNE adducts-** LC-MS characterization of the reaction products between carnosinol and HNE. Reaction products were formed by incubating carnosinol with HNE for 24h at 37°C.

Upper panel - MS/MS spectrum of the Schiff base at *m/z* 351 (collision energy 25V).

Bottom panel - MS/MS spectrum of the Michael adduct at *m/z* 369 (collision energy 35V);

Proposed structures of the ion fragments were calculated by using Mass Frontier Spectral Interpretation Software (Thermo Scientific)

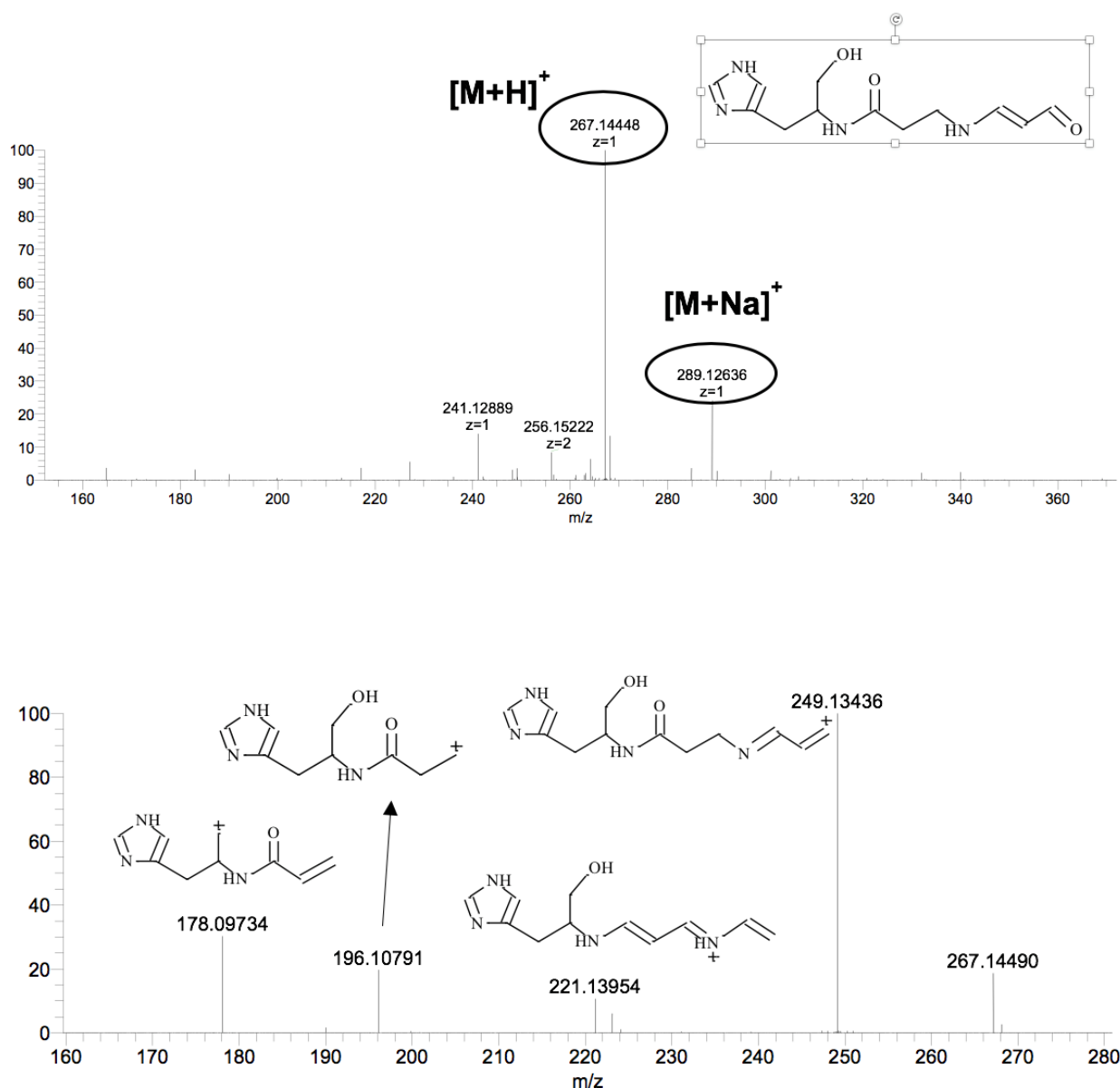
## Supplemental Figure 2



**Supplementary Figure 2. Carnosinol-MGO adducts.** Mass spectra of the reaction mixture of carnosinol and MGO after 24h of incubation at 37°C.

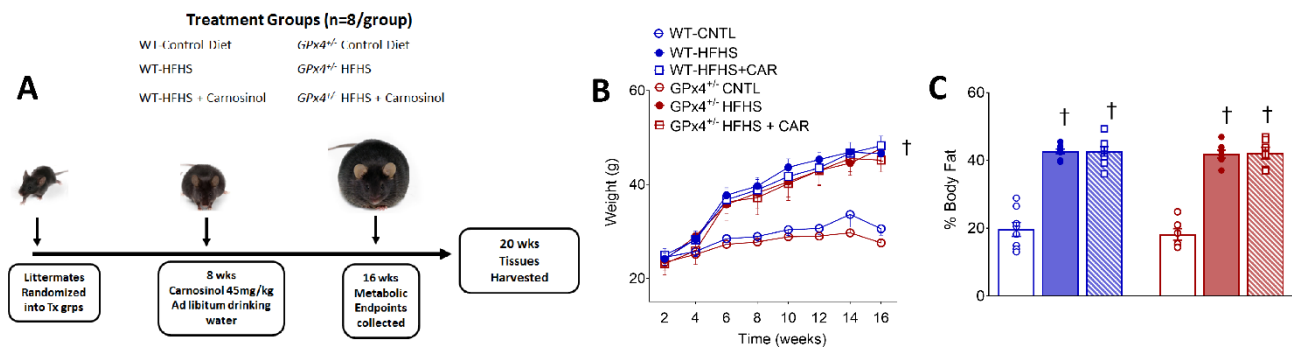
A) mass spectrum of the reaction mixture of carnosinol and MGO characterized by the peaks at  $m/z$  213 attributed to carnosinol and at  $m/z$  472 attributed to the MOLD (Methylglyoxal-derived Lysine Dimer) like structure. B) MS/MS spectrum of the MOLD adduct at  $m/z$  472 (collision energy 35V).

### Supplemental Figure 3



**Supplementary Figure 3. Carnosinol-MDA adducts-** Mass spectrometric identification and characterization of the reaction product between carnosinol and MDA. Reaction products were formed by incubating carnosinol with MDA for 24h at 37°C. Upper panel - MS spectrum of the reaction mixture characterized by the most abundant ion at  $m/z$  267 which is attributed to the carnosinol N-propenal adduct. The corresponding cationized (sodium) adduct is detectable at  $m/z$  289. Bottom panel - MS/MS spectrum of the adduct ion at  $m/z$  267 (collision energy 35V); Proposed structures of the ion fragments were calculated by using Mass Frontier Spectral Interpretation Software (Thermo Scientific).

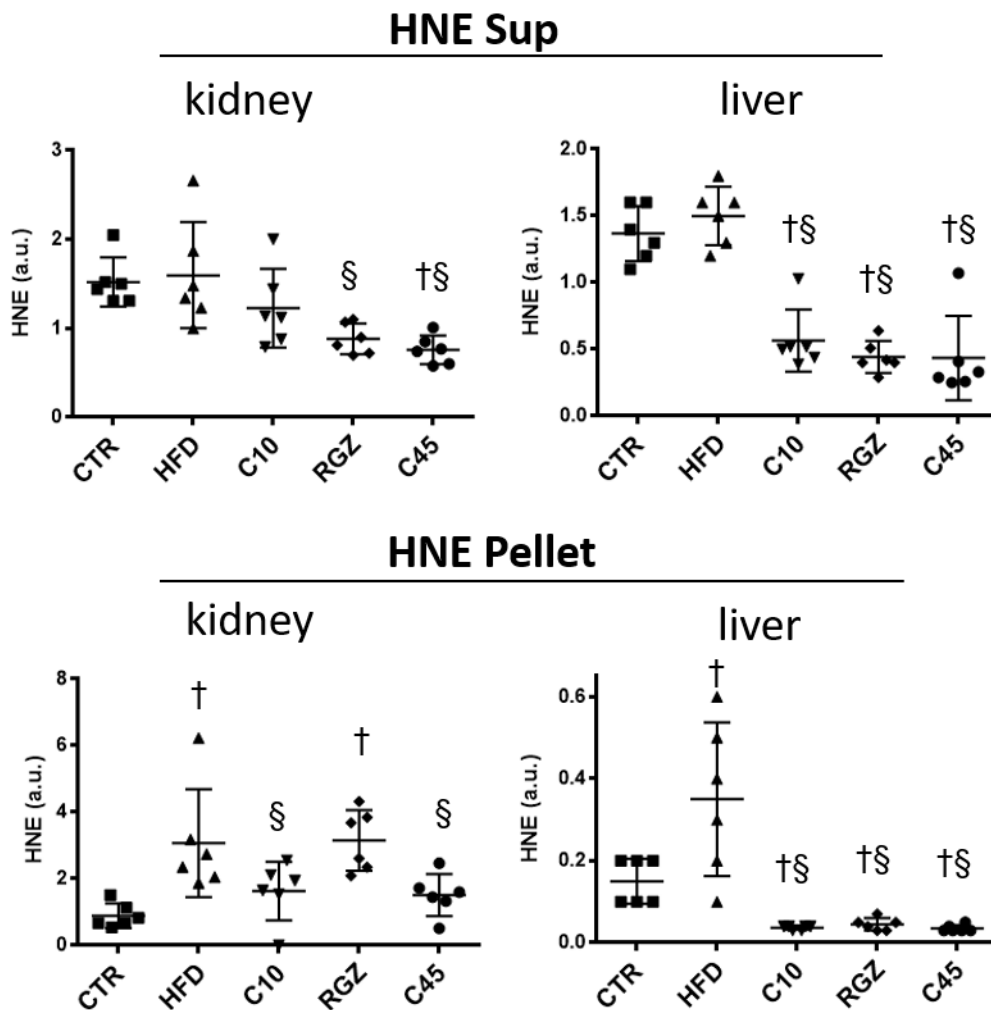
## Supplemental Figure 4



**Supplemental Figure 4. Study design and effect of carnosinol on body weight and adiposity in mouse models of diet-induced obesity.** The overall study design to examine the effect of carnosinol on HFHS diet-induced obesity in WT and *GPx4*<sup>+/-</sup> mice is shown in (A). Body weight gain over the course of the intervention period (B) and the fat mass of the mice at termination of the study (C) are also shown.



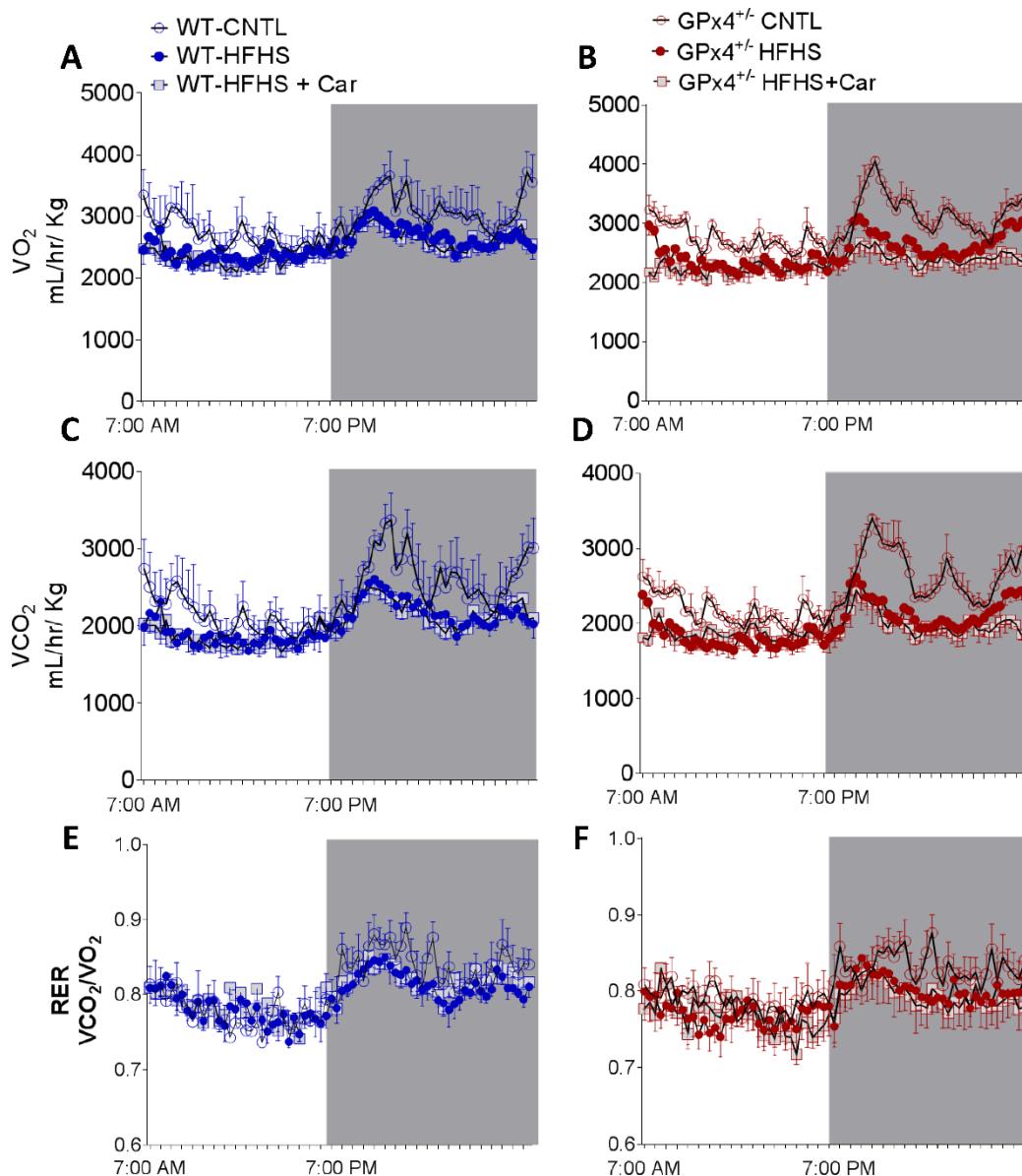
## Supplemental Figure 5



### Supplemental Figure 5. HNE-adduct levels in subcellular Kidney and Liver fractions.

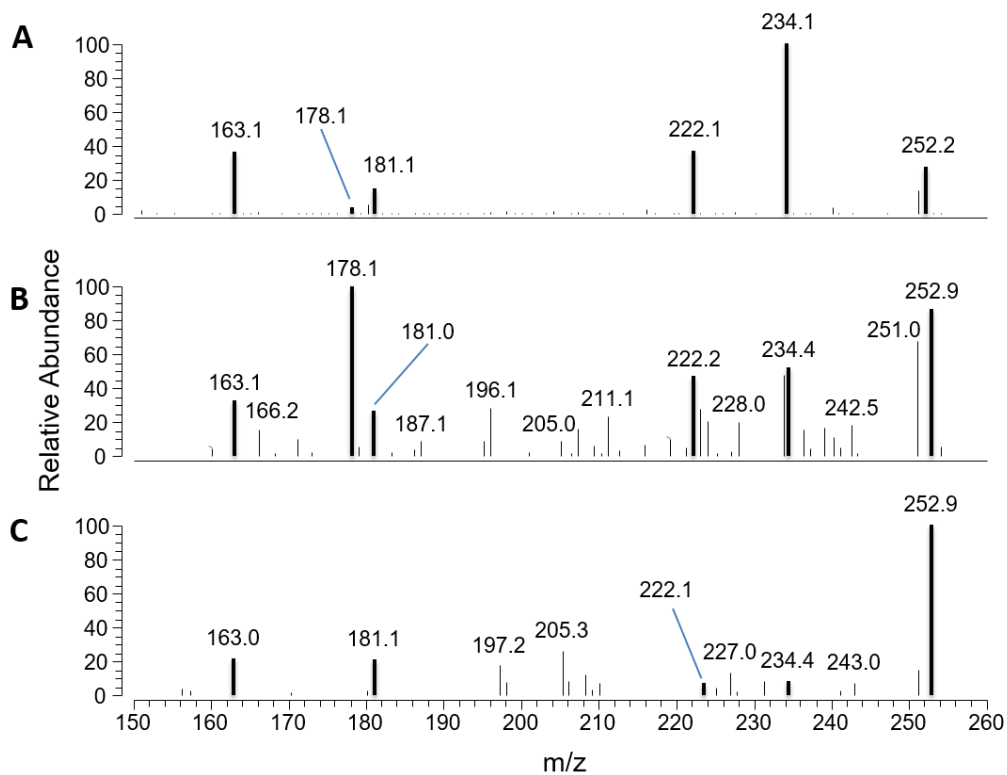
The levels of HNE-protein adducts formed in response to either Hi Fructose diet (HFD) alone, or combined with low (10 mg/kg) or high (45 mg/kg) dose carnosinol and rosiglitazone (RGZ) in drinking water is shown quantified in subcellular fractions from Kidney and Liver. In the top set of panels are levels of HNE-adducts in Supernatant fractions (Triton X-100 soluble fraction), and in the lower set of panels are levels of HNE from Pellet fractions (detergent insoluble/lipid-raft fraction) from these tissues. Data are reported as means  $\pm$  S.D. for three independent experiments performed in duplicate. † $P < 0.01$  vs. Control Diet; § $P < 0.01$  vs. HFD alone.

## Supplemental Figure 6



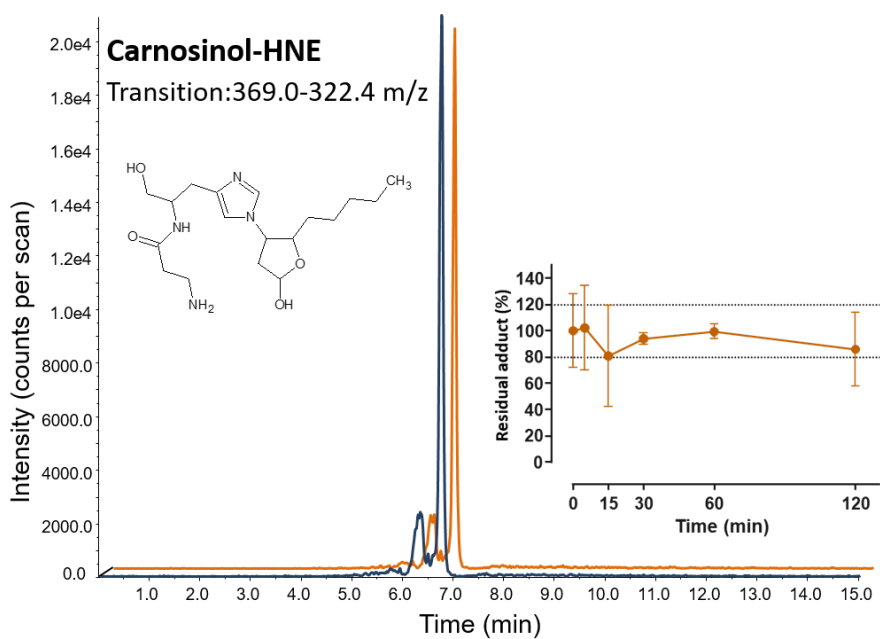
**Supplemental Figure 6. Energy expenditure.** Whole-body  $VO_2$  (A, B) and  $VCO_2$  (C, D) were measured during a 4-day interval in week 14 of the dietary intervention in mice from each of the 6 groups used in this study. From these values, respiratory exchange ratio (RER) was calculated for each of the groups (E, F). Data are from n=4 mice/group.

## Supplemental Figure 7



**Supplemental Figure 7. Tandem mass spectra of ion at 269.1 m/z in the following samples:** A) carnosinol-acrolein adduct in phosphate buffer used as reference B) peak at 10.3 minutes in rat liver homogenate as shown in bottom panel of Fig. 6J, and C) peak at 10.2 minutes shown in WT-HFHS + Car group from Fig. 6J.

## Supplemental Figure 8



**Supplemental Figure 8. Stability of carnosinol in human serum:** Shown in this panel are representative LC-MS chromatograms of carnosinol-HNE adducts in human serum with time. The blue and tan-colored peaks are representative of one experiment showing the adduct at beginning and end of incubation. Total adduct concentration in human serum over time is shown in the panel-inset right (N=4).